Notes

Microstructure and Thermal Property of Isotactic Poly(3-methyl-1-butene) Obtained Using the C_2-Symmetrical Zirconocene/MAO Catalyst System

Wei Hu,[†] Hideaki Hagihara,[‡] and Toshikazu Miyoshi*,[†]

Nanotechnology Research Institute and Research Institute for Innovation in Sustainable Chemistry, National Institute for Advanced Industrial Science and Technology, Central 5-1, Higashi 1-1-1, Tsukuba, Ibaraki 305-8565, Japan

Received September 13, 2006

Revised Manuscript Received January 11, 2007

Introduction

Isotactic poly(3-methyl-1-butene) (iP3M1B) has been synthesized and studied since the 1950s because it is a promising material with a high thermal property; the iP3M1B synthesized using the traditional Ziegler−Natta catalyst shows a high T_m of 305 °C, which is much higher than that of the commercially available isotactic poly(4-methyl-1-pentene) (T_m = 245 °C).[1−3]

Recently, several types of homogeneous catalyst based on group 4 metallocene catalysts have also been investigated for the polymerization of 3M1B. However, the thermal property of the obtained products is not satisfactory compared with those of products obtained using Ziegler−Natta catalysts.[4,5] For example, Borriello et al. reported that iP3M1B synthesized using C_2-symmetric metallocenes gives T_m as low as 280 °C.[4]

Microstructural parameters such as regioregularity, isotacticity, and molecular weight of isotactic polypropylene (iPP) influence T_m.[6−8] Nevertheless, the analysis of such structural parameters of iP3M1B has seldom been successful because of the limited solubility of iP3M1B in almost all types of available solvent.[4,5] There is only one detailed report on the treatment of iP3M1B with a low isotacticity *mm* = 74%.[9]

There have been several advancements in the melt-state NMR analysis of insoluble polymers and branch content characterization up to 200 °C.[10−13] Very recently, we succeeded in obtaining high-resolution melt-state NMR spectra at a very high temperature above 300 °C for microstructural characterization.[14]

In this work, we investigate three types of C_2-symmetric homogeneous metallocene catalyst, namely, *rac*-dimethylsilylenebis(1-indenyl)zirconium(IV) dichloride ((DMSBI)$ZrCl_2$), *rac*-dimethylsilylenebis(2-methyl-1-indenyl)zirconium(IV) dichloride ((DMSBMI)$ZrCl_2$), and *rac*-dimethylsilylenebis(2-methyl-4-phenyl-1-indenyl)zirconium(IV) dichloride ((DMSBMPI)$ZrCl_2$), for iP3M1B synthesis and study the thermal properties and stabilities of the products using DSC and TGA, respectively. It is shown iP3M1B synthesized using (DMSBMI)$ZrCl_2$/MAO exhibits high thermal stability with reasonable productivity. Moreover, melt-state NMR analysis at high temperatures above T_m will directly reveal how microstructures influence the thermal properties of the products.

* Corresponding author. E-mail: t-miyoshi@aist.go.jp.
[†] Nanotechnology Research Institute.
[‡] Research Institute for Innovation in Sustainable Chemistry.

Experiments

Materials. 3-Methyl-1-butene (3M1B) with a purity of >98% was commercially obtained from Tokyo Kasei Kogyo Co, Ltd. (DMSBI)$ZrCl_2$, (DMSBMI)$ZrCl_2$, and (DMSBMPI)$ZrCl_2$ were purchased from Wako Chem. Co. MAO ([Al] = 6.7 (wt %) in toluene) was received from Tosoh Chem. Co. These materials were used without further purification. Toluene from Wako Chem. Co. was distilled in nitrogen atmosphere and preserved with molecular sieves 3A. The other reagents were obtained commercially and used as received.

Polymerization. iP3M1B was synthesized in a 200 mL three-necked glass bottle equipped with a magnetic stirrer. The reaction equipment was evacuated for half an hour and filled with nitrogen before polymerization. MAO toluene solution (5 mL) was added to 30 mL of toluene under nitrogen. 3M1B was added to this solution after the reactor was again evacuated. Finally, 20 μmol of catalyst was injected into the bottle and stirred at different temperatures for different times. The polymerization was terminated by adding methanol, upon which a white compound precipitated. Hydrochloric acid (~36%) was added to react with the remaining catalyst. More methanol was added, and the mixture was stirred overnight to fully precipitate the polymer. The precipitated polymer was filtered off, washed with methanol, and dried at 60 °C under vacuum for at least 4 h to evaporate the solvents. White iP3M1B powder was obtained. We denote the iP3M1B samples synthesized under different polymerization conditions samples 1−15, as listed in Tables 1 and 2. Sample 15 was fractionated by Soxhlet extraction using boiling *n*-heptane for 12 h to confirm the purity of our products. Only 0.2 wt % appears as a soluble part, which is significantly less than that of iP3M1B (7.1%) synthesized by Ziegler−Natta catalysis.[3] Thus, we performed further investigations of the microstructures and thermal properties of samples 1−15 without fractionation.

DSC and TGA Analyses. DSC analysis was performed using Seiko SSC/6000 (DSC 6000) in a N_2 atmosphere at a heating rate of 10 °C/min. TGA analysis was performed on Seiko Instrument Inc ExSTAR 6000 (TG/DTA 6200) at a heating rate of 10 °C/min.

NMR Analysis. The melt-state ^{13}C magic-angle spinning (MAS) NMR analysis at very high temperatures was conducted on a BRUKER AVANCE 300 spectrometer equipped with a 4 mm high-temperature MAS NMR probe. The samples (30−40 mg) were packed into the central part of the NMR rotors, and open spaces were blocked with Teflon tape. N_2 gas was used as the MAS gas source to protect NMR coils and probes. The actual temperature of the sample surroundings in the NMR machine was calibrated carefully using the temperature dependence of the ^{207}Pb chemical shift of $Pb(NO_3)_2$.[15] The frequency of MAS was set to 3500 ± 5 Hz. The ^1H and ^{13}C carrier frequencies are 300.1 and 75.6 MHz, respectively. We used the ^{13}C direct polarization (DP) method with a 90° pulse length of 4.5 μs under high-power ^1H continuous-wave (CW) decoupling at a field strength of 50 kHz in the detecting period. The CH signal of adamantine (29.5 ppm) was set as an external reference for the chemical shift. The recycle time and total experimental spectrum were 500 ms and 3 h, respectively, for each spectrum. More details are shown elsewhere.[14]

10.1021/ma062121a CCC: $37.00
Published on Web 02/10/2007

Table 1. Polymerization of 3-Methyl-1-butene Using C_2-Symmetric Metallocene Catalyst[a] and Thermal Properties, Stabilities, and Microstructures of Products

sample	catalyst[b]	monomer mass	yield (g)	yield (%)	T_m (°C)	T_{d5} (°C)	isotacticity (%)	regiodefect(%)	$\bar{M}_n$ (g/mol)
1	(DMSBI)$ZrCl_2$	9.4	1.5	16.0	285	390	>97	0.9 ± 0.4[c]	14 000 ± 3000[c]
2	(DMSMBI)$ZrCl_2$	7.4	2.5	33.8	299	406	94	0	17 000 ± 3000[c]
3	(DMSBMPI)$ZrCl_2$	6.2	0	0					

[a] Polymerization conditions: 20 μmol of catalyst, 30 mL of toluene, 5 mL of MAO ([Al] = 6.7 (wt %) in toluene), 20 °C for 3 h. [b] Abbreviations: (DMSBI)$ZrCl_2$ = *rac*-dimethylsilylenebis(1-indenyl)zirconium(IV) dichloride; (DMSBMI)$ZrCl_2$ = *rac*-dimethylsilylenebis(2-methyl-1-indenyl)zirconium(IV) dichloride; (DMSBMPI)$ZrCl_2$ = *rac*-dimethylsilylenebis(2-methyl-4-phenyl-1-indenyl)zirconium(IV) dichloride. [c] Experimental errors arise from S/N ratios in the spectra.

Table 2. Polymerization of 3M1B Using *rac*-Dimethylsilylenebis(2-methyl-1-indenyl)zirconium(IV) Dichloride/MAO ([Al] = 6.7 wt % in Toluene) and Thermal Properties, Stabilities, and Microstructures of Products

sample	monomer mass (g)	T_p (°C)	t_p (h)	yield (g)	yield (%)	T_m (°C)	T_{d5} (°C)	isotacticity (*mm* %)	$\bar{M}_n$ (g/mol)[a]
4	7.1	50	3	3.2	45.1	292	389	91	14 000 ± 4000
2	7.4	20	3	2.5	33.8	299	406	94	17 000 ± 3000
5	7.7	20	12	4.1	53.2	299	395		14 000 ± 4000
6	8.2	20	55	5.5	67.1	301	400		
7	5.2	0	3	1.2	23.1	300	396	95	14 000 ± 4000
8	6.0	0	12	3.8	63.3	301	398		
9	12.1	0	55	11.5	95.0	303	404		
10	7.0	−20	3	1.5	21.4	302	405	95	
11	7.2	−20	24	4.1	56.9	302	395		13 000 ± 3000
12	6.6	−20	65	5.2	78.8	303	414	97	23 000 ± 7000
13	6.7	−40	3	0.2	3.0	302	407	96	9000 ± 2000
14	6.4	−40	24	0.6	9.4	303	404		
15	8.8	−40	100	7.0	79.5	304	399	96	20 000 ± 7000

[a] Experimental errors arise from the S/N ratios in the NMR spectra.

Results and Discussion

Three C_2-symmetric homogeneous catalysts, namely, (DMSBMI)$ZrCl_2$, (DMSBI)$ZrCl_2$, and (DMSBMPI)$ZrCl_2$, were employed for the polymerization of 3M1B in combination with MAO as a cocatalyst. The results of the polymerization are summarized in Table 1. The productivity of sample 3 with (DMSBMPI)$ZrCl_2$/MAO is almost zero, although (DMSBMPI)-$ZrCl_2$ produces iPP with relatively high thermal property and productivity compared with (DMSBMI)$ZrCl_2$ and (DMSBI)-$ZrCl_2$.[6] There is a bulky side group, isopropyl, on 3M1B. The reason for the above result might be that the bulky structure of the ligand hinders the insertion of the 3M1B monomer, which is also bulky.[16,17]

The syntheses using (DMSBI)$ZrCl_2$ and (DMSBMI)$ZrCl_2$ yield reasonable amounts of samples (16% and 34%, respectively). T_m of sample 2 is 299 °C, which is higher than that for sample 1 (285 °C). In the case of iPP, microstructures such as stereo- and regiodefects and molecular weight largely affect the T_m of the products.[6,18] Therefore, it is scientifically important to investigate the microstructure of iP3M1B samples showing different thermal behaviors.

Figure 1 shows ^{13}C melt-state NMR spectra of iP3M1B samples 1 and 2 at 315 °C. There are four main peaks for both of them, C2, C1, C3, and C4, which are assigned to main-chain CH, CH_2, side-chain CH, and two CH_3 carbons, respectively.[9] Almost every carbon resonance is a single resonance with minor shoulder components at the bottom. The previous solution-state ^{13}C NMR analysis and chemical shift calculations for a low-isotacticity iP3M1B sample demonstrated that the ^{13}C C3 signal is resolved into multiple peaks assigned to *mm*, *mr*, and *rr* structures from the downfield side to the upfield side in the range of ∼1 ppm.[9] On the other hand, the C3 signal in the melt-state NMR analysis is unresolved because of the low spectral resolution, but the asymmetric shape consists of the major peak at 30.7 ppm and a very small shoulder peak at ∼30.3 ppm. The

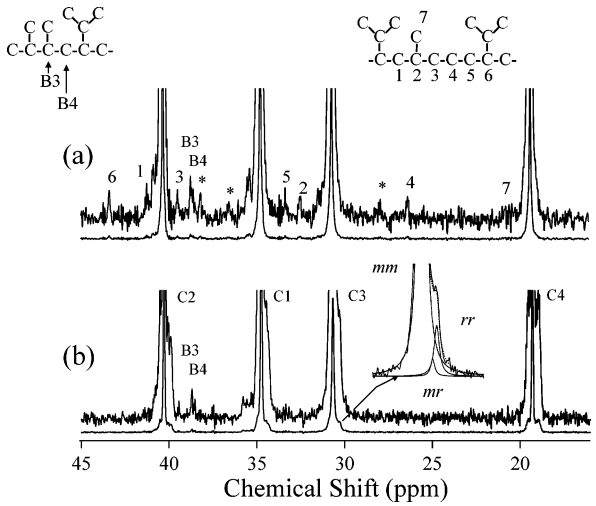

Figure 1. Melt-state ^{13}C NMR spectra for iP3M1B samples 1 (a) and 2 (b) at 315 °C. For both cases, the upper spectrum is enlarged 10 times. The regiodefect and end-group structures and signal assignments are also shown.[4] The line-shape analysis of the C3 signal is also shown using three Lorentzian peaks.

observed shoulder is attributed to the overlapping stereodefect signals, *mr* and *rr*. The obtained ^{13}C NMR line shape for the C3 signal is assumed to be fitted by three Lorentzian peaks, which are assigned to *mm*, *mr*, and *rr* structures, at 30.7, 30.4, and 30.2 ppm, respectively. Consequently, it is shown that iP3M1B samples 1 and 2 exhibit isotacticities of >97 and 94%, respectively. The fitted peaks for the C3 signals of sample 2 are inserted in Figure 1b. These results indicate that the isospecificity of (DMSBI)$ZrCl_2$ is slightly better than that of (DMSBMI)$ZrCl_2$.

The spectra also show two typical signals corresponding to the end groups of oligomers reported in the solution-state NMR

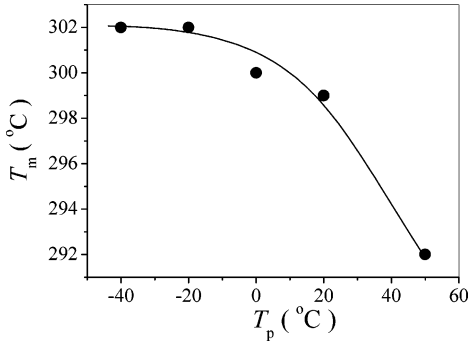

Figure 2. Relationship between T_p and T_m of synthesized iP3M1B when polymerization time was 3 h.

analysis.[4] The proposed end-group structure and assignment of the signals B3 and B4 are also shown in Figure 1. The end-group intensities for sample 1 are slightly higher than those for sample 2. In addition, there is another set of weaker peaks indicating heterogeneous structures arising from regiodefects in sample 1. Such peaks were assigned to the structure shown by the right-hand scheme in Figure 1.[4] There are also some other minor peaks (*), which we could not assign, that may correspond to other regiodefects or end-group structures. On the other hand, no signals corresponding to the regiodefect structures are observed for sample 2. These experimental findings indicate that the regiospecificity of (DMSBMI)$ZrCl_2$ is better than that of (DMSBI)$ZrCl_2$.

In our previous work, we demonstrated that B3 and regiodefect ^{13}C signals in the low-molecular-weight iP3M1B sample with an average molecular weight ($\bar{M}_n$) = 2400 show similar NOE and relaxation behaviors to the main signals C1, C2, C3, and C4.[14] Under such conditions, the obtained NMR signals at a recycle delay before a ^{13}C full relaxation allow us to estimate defect concentration and $\bar{M}_n$.[12,14] We evaluated $\bar{M}_n$ and the regiodefect concentration using the B3 and No. 6 signals (Figure 1a) and C1 as a reference. Consequently, it was found that samples 1 and 2 show $\bar{M}_n = 14\,000 \pm 3000$ and $17\,000 \pm 3000$, respectively, and the former includes regiodefects at a concentration of $0.9 \pm 0.4\%$.

Sample 1 shows slightly high isotacticity and $\bar{M}_n$ compared with sample 2. Nevertheless, the former includes regiodefects at a concentration of 0.9%. This structural difference may be the main reason for the lower T_m. Thus, the effect of regiodefects on T_m has been investigated in propylene polymerization.[18−20] Pavan et al. reported presence of head-to-head chain irregularities at 1% decreased the T_m of iPP about 10 °C.[19] This tendency is consistent with our result and supports our conclusion.

We also aim at the synthesis of iP3M1B at even higher T_m using (DMSBMI)$ZrCl_2$. There are two other factors, polymerization temperature and time, which should be examined to improve T_m, the isotacticity, and molecular weight of iP3M1B.[8] 3M1B was polymerized using the (DMSBMI)$ZrCl_2$/MAO system at various polymerization temperatures (T_p = 50 to −40 °C) and times (t_p = 3 to 100 h). The conditions and main results are shown in Table 2. T_m increases to more than 300 °C, for instance, 304 °C for synthesis 15, which is the highest T_m for iP3M1B synthesized using homogeneous metallocene catalysts and is very close to that of products synthesized using Ziegler−Natta catalysts (305 °C).[1] It could be observed that at the same polymerization temperature (T_p) the T_m of iP3M1B obtained after a longer polymerization time (t_p) is always higher than the T_m of those produced with a shorter polymerization time. In addition, Figure 2 shows the relationship between the T_p and T_m of iP3M1B obtained at a t_p of 3 h. It is apparent that T_m increases with decreasing T_p. Furthermore, we investigated the 5% weight-loss temperature (T_{d5}) for all the samples. Almost all the T_{d5} data are very high (>400 °C). However, the T_{d5} data are more scattered than the T_m data.

The ^{13}C melt-state NMR spectrum of *i*P3M1B polymerized at various T_p and t_p values were obtained. All the spectra show no regiodefects in the iP3M1B products obtained using the (DMSBMI)$ZrCl_2$/MAO system under all conditions. When t_p is fixed at 3 h, the C3 signals clearly demonstrate that isotacticity increases with decreasing T_p. For instance, the ^{13}C melt-state spectrum and analysis data of the C3 signals of the samples synthesized at $T_p = -40$ and 50 °C for 3 h shown in Figure 3a show *mm* = 96 and 91%, respectively.[9] The other results are also listed in Table 2. In addition, we paid attention to the end-group (B3) intensities and $\bar{M}_n$. Figure 3b shows the spectra of the end-group signals, the intensities of which are, of course, very small. $\bar{M}_n$ is estimated to be $14\,000 \pm 4000$ and 9000 ± 2000 at 50 and −40 °C at t_p = 3 h, respectively. The other $\bar{M}_n$ values are also listed in Table 2. Molecular weight decreases significantly as a function of T_p at temperatures below −20 °C. It is well understood that iPP with higher molecular weight always leads to higher T_m.[8] Therefore, the observed tendency in molecular weight as a function of T_p is opposite to that of T_m shown in Figure 2. It is, therefore, concluded that an increase in isotacticity mainly contributes to the observed T_m tendency (Figure 2).

As another interesting point, the dependence of $\bar{M}_n$ on t_p changes in accordance with T_p. At 20 °C, $\bar{M}_n$ is unchanged or, rather, decreases with increasing t_p. This is normal behavior in nonliving polymerization. At a low T_p of −40 °C, however, $\bar{M}_n$ markedly increases with increasing t_p ($\bar{M}_n = 9000 \pm 2000$, 3 h, and $20\,000 \pm 7000$, 100 h). Our explanation for this is as follows: The catalyst system showed high activity even in the early stage of polymerization (such as 3 h) at 20 °C. At low T_p,

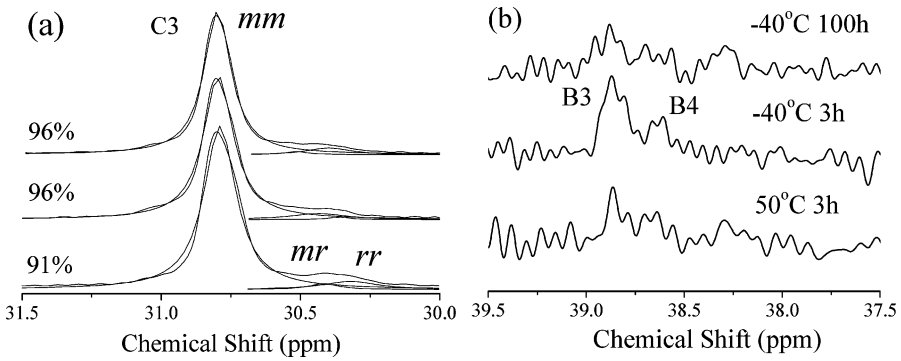

Figure 3. (a) Expanded ^{13}C melt-state NMR spectra of C3 (a) and B3 and B4 (b) signals of iP3M1B synthesized at 50 and −40 °C for 3 h and at −40 °C for 100 h. The three fitted peaks showing *mm*, *mr*, and *rr* peaks are also given.

however, the productivity in a short polymerization time is considerably low (3.0% and 9.4% for 3 and 24 h, respectively). Meanwhile, the productivity exponentially increases with increasing t_p (100 h, 79.5%). Therefore, the early stage of polymerization at low T_p seems to be an induction period. This induction period of polymerization may be due to the slow initiation of the zirconocene catalyst. Thus, polymers obtained in the early stage of polymerization are expected to contain a considerable amount of oligomeric products and as a result show low $\bar{M}_n$ in the initial period at low T_p.

Conclusions

We performed systematic investigations of the synthesis, thermal properties, and microstructures of iP3M1B. We used three C_2 methallocene catalysts, namely, (DMSBMPI)$ZrCl_2$, (DMSBI)$ZrCl_2$, and (DMSMBI)$ZrCl_2$ with MAO, for the synthesis of iP3M1B. Among the three catalysts, (DMSMBI)-$ZrCl_2$/MAO yields the product iP3M1B with the highest T_m of 299 °C. It was revealed by melt-state NMR analysis that the sample synthesized with (DMSMBI)$ZrCl_2$ shows a high regiospecificity, which is the main reason for the high T_m. In addition, it was also found by melt-state NMR analysis that a low T_p of −40 °C and a long t_p of 100 h are highly effective in further increasing the stereospecificity of (DMSMBI)$ZrCl_2$ catalyst and the $\bar{M}_n$ of the products, respectively. Consequently, bulk T_m also increases to 304 °C, which is similar to the maximum T_m of the sample synthesized using Ziegler Natta catalyst.

Through this work, we demonstrated that melt-state NMR analysis yields important microstructure information even for insoluble polymers, similar to that obtained by solution-state NMR analysis, although melt-state NMR analysis still suffers from a lower spectral resolution.

Acknowledgment. The authors thank the New Energy and Industrial Technology Development Organization (NEDO) and the Japan Society for the Promotion of Science (JSPS) for support of this work.

References and Notes

(1) Kirshenbaum, I.; Feist, W. C.; Issacson, R. B. *J. Appl. Polym. Sci.* **1965**, *9*, 3023−3031.
(2) Lopez, L. C.; Wilkes, G. L.; Stricklen, P. M.; White, S. A. *Rev. Macromol. Chem. Phys.* **1992**, *C32*, 301−406.
(3) Atarashi, Y. *J. Polym. Sci., Part A-1* **1970**, *8*, 3359−3366.
(4) Borriello, A.; Busico, V.; Cipullo, R. *Macromol. Rapid Commun.* **1996**, *17*, 589−597.
(5) Rishina, L. A.; Galashina, N. M.; Nedorezova, P. M.; Klyamkina, A. N.; Aladyshev, A. M.; Tsvetkova, V. I.; Kleiner, V. I. *Polym. Sci., Ser. A* **2003**, *45*, 209−214.
(6) Spaleck, W.; Kuber, F.; Winter, A.; Rohrmann, J.; Bachmann, B.; Antberg, M.; Dolle, V.; Paulus, E. F. *Organometallics* **1994**, *13*, 954−963.
(7) Stehling, U.; Diebold, J.; Kirsten, R.; Röll, W.; Bringtzinger, H. H.; Jüngling, S.; Mülhaupt, R.; Langhauser, F. *Organometallics* **1994**, *13*, 964−970.
(8) Rieger, B.; Mu, X.; Mallin, D. T.; Rausch, M. D.; Chien, J. C. W. *Macromolecules* **1990**, *23*, 3559−3568.
(9) Asakura, T.; Nakayama, N. *Polym. Commun.* **1991**, *32*, 213−216.
(10) Thakur, K. A. M.; Newmark, R. A.; Kuehn, N. T.; Gregar, T. Q. *Macromolecules* **2003**, *36*, 719−723.
(11) Isbester, P. K.; Brandt, J. L.; Kestner, T. A.; Munson, E. J. *Macromolecules* **1998**, *31*, 8192−8200.
(12) Pollard, M.; Klimke, K.; Graf, R.; Spiess, H. W.; Wilhelm, M.; Sperber, O.; Piel, C.; Kaminsky, W. *Macromolecules* **2004**, *37*, 813−825.
(13) Alamo, R. G.; Blanco, J. A.; Carrilero, I.; Fu, R. *Polymer* **2002**, *43*, 1857−1865.
(14) Hu, W.; Hagihara, H.; Miyoshi, T. Manuscript in preparation.
(15) Bielecki, A.; Burum, D. P. *J. Magn. Reson. A* **1995**, *116*, 215−220.
(16) Burger, P.; Hortmann, K.; Brintzinger, H. H. *Makromol. Chem., Macromol. Symp.* **1993**, *66*, 127−139.
(17) Kaminsky, W.; Engehausen, R.; Zoumis, K.; Spaleck, W.; Rohrmann, J. *Makromol. Chem.* **1992**, *193*, 1643−1651.
(18) Deng, H.; Winkelbach, H.; Taeji, K.; Kaminsky, W.; Soga, K. *Macromolecules* **1996**, *29*, 6371−6376.
(19) Pavan, A.; Provasoli, A.; Moraglio, G.; Zambelli, A. *Makromol. Chem.* **1977**, *178*, 1099−1109.
(20) Grassi, A.; Zambelli, A.; Resconi, L.; Albizzati, E.; Mazzocchi, R. *Macromolecules* **1988**, *21*, 617−622.

MA062121A